ARCHIVES
of
FOUNDRY ENGINEERING
10.24425/afe.2021.136076
Published quarterly as the organ of the Foundry Commission of the Polish Academy of Sciences

ISSN (2299-2944)
Volume 21
Issue 1/2021
37 – 50
6/1

Hot Dipping of Chromium Low-alloyed Steel in Al and Al-Si Eutectic Molten Baths

G. M. Attia, W. M. A. Afify *, M. I. Ammar
Metallurgical and Materials Engineering Department,
Faculty of Petroleum and Mining Engineering Suez University, Egypt
* Corresponding author: Email address: Engwalaaatef@gmail.com

Received 10.08.2020; accepted in revised form 23.12.2020

Abstract

Chromium low alloyed steel substrate was subjected to aluminizing by hot dipping in pure aluminium and Al-Si eutectic alloy at 750°C and 650°C respectively, for dipping time up to 45 minutes. The coated samples were subjected for investigation using an optical microscope, scanning electron microscopy (SEM), Energy-dispersive X-ray analyzer (EDX) and X-ray diffraction (XRD) technique. Cyclic thermal oxidation test was carried out at 500°C for 72 hours to study the oxidation behaviour of hot-dipped aluminized steel. Electrochemical corrosion behavior was conducted in 3wt. %NaCl aqueous solution at room temperature. The cyclic thermal oxidation resistance was highly improved for both coating systems because of the formation of a thin protective oxide film in the outermost coating layer. The gain in weight was decreased by 24 times. The corrosion rate was decreased from 0.11 mmpy for uncoated specimen to be 2.9 x10^{-3} mmpy for Aluminum coated steel and 5.7x 10^{-3} mmpy for Al-Si eutectic coated specimens. The presence of silicon in hot dipping molten bath inhabit the growth of coating intermetallic layers, decrease the total coating thickness and change the interface boundaries from tongue like shape to be more regular with flatter interface. Two distinct coating layers were observed after hot dipping aluminizing in Al bath, while three distinct layers were observed after hot dipping in Al-Si molten bath.

Keywords: Coating, Hot dipping, Aluminizing, Chromium low alloyed steel

1. Introduction

Plain and low alloyed steel are considered the most demanding materials for multipurpose applications, because of their low cost and wide varity of properties that play a vital role in alloy design, heat treatment, and forming operations [1]. Steel has many physical advantages such as high strength, elasticity, ductility, and toughness; however, it has many limitation properties like low corrosion and oxidation resistance at high temperature, low fatigue strength in addition to susceptibility to brittle fracture and buckling [2]. The modification was required to enhance the corrosion and oxidation properties by alloying the steel with different elements such as chromium and nickel, but this increases the cost of material and limits width of the processing window [1]. Surface modification of the steel is an alternative choice for an expensive alloy steel material [3]. The surface modification can be applied using a suitable method. When an appropriate technique is used and correctly done, many properties of the steel such as corrosion, oxidation, mechanical and wear resistance can be increased [4, 5]. Coating considered a very important technique to determine the efficiency of the material. Surface coating is a cost-effective and simple technique which acts as a protective layer when applied to the surface of the substrate [6]. Hot-dip aluminizing is less expensive and an effective coating process to protect steels from oxidation and corrosion [1, 7, 8, 9, 10]. When applying aluminium as a coating material on the surface of the steel, it can form a corrosion resistance layer [11, 12]. Formation of a continuous alumina layer can protect the steel from oxidation, sulfidation and degradation in seawater [13]. The presence of silicon in hot dipping molten aluminium bath improve the fluidity of molten metal and provide the aluminide layer better mechanical properties, good adherence and high-temperature corrosion [14]. The addition of Si to hot dipping molten bath was found to restrict the growth rate of intermetallic layer and subsequently decrease the thickness of the brittle phases, improve formability and a flattening of the coating/substrate interface [15, 16]. The aim of this work is to improve both high oxidation resistance and corrosion resistance for chromium low alloyed-steel. Chromium low alloyed steel was chosen in this work because there are very little works were published about this alloy in addition, this alloy is normally used in some of the high-temperature applications (boiler tubes) [17].

In the present study, chromium low alloyed steel was aluminized by using pure Al and Al-Si eutectic alloy melts. The thickness and microstructural details of the coated layers were investigated. The cyclic thermal oxidation resistance and corrosion behaviour of coated and uncoated samples were also be tested.

2. Experimental

2.1. Materials

The chemical composition of chromium low alloyed steel grade used in the present work is given in table (1). The substrate material was machined and cut in a cylindrical shape having 10 mm length and 20 mm in diameter. The specimens were grounded using a set of emery papers (till grade 1200) and then cleaned by acetone.

Tables (2) and (3) represent the chemical nominal compositions of aluminium and aluminium- 11.7% silicon eutectic alloy which used in hot dipping aluminizing process.

Table 1.
The chemical composition, in wt. %, of chromium low alloyed steel grade

Elements (wt. %)									
C%	Si%	Mn%	P%	Cu%	Ti%	Ni%	Nb%	Cr%	Fe%
0.208	0.297	0.67	0.01	0.046	0.0058	0.119	0.027	3.0	Balance

Table 2.
Chemical composition, in wt. %, of commercial pure Al

Elements (wt.%)						
Al	Cu	Fe	Mn	Si	Zn	Residuals
99-99.95%	0.05-0.2%	0.95% max	0.05% max	0.95% max	0.10% max	0.15% max

Table 3.
Chemical composition, in wt. % of Al- 11.7 % Si

Elements (wt.%)					
Si	Mg	Zn	Fe	Al	Residuals
7-12%	0.05%	0.1%	0.95%	Balance	0.15% max

2.2. Fluxing

Steel specimens were degreased and descaled to provide a fresh surface to facilitate contact with molten bath materials. The fluxing solution used in the present study was prepared by adding equal amounts of NaCl and KCl to the water forming a 25% weight percentage solution [2]. The specimens were immersed in flux - solution for 3 minutes time interval, then rinsed and dried just before hot dipping. Fluxing was applied on surface to improve the wetting between substrate and molten melt and promote the dissolution of surface darts and surface oxides present on the steel substrate.

2.3. Hot dipping process

Three samples were prepared for every dipping time. After hot dipping, specimens were cross sectioned and mounted in epoxy resin. The mounted specimens were subjected to grinding and polishing using classical preparation methods. The polished specimens were selectively etched using Nital 3% solution to reveal the matrix (3ml HNO_3+97ml ethyl alcohol) and Killer etcher (0.5ml HF+1.5ml HCL and 1ml HNO_3) to reveal the microstructure details of coating layer [18].

2.4. Microstructure examinations

Microstructure examinations and layer thickness measurements were carried out by using Olympus optical microscope type (OLYMPUS DP73) fitted with micrometer. The layer thicknesses of coated specimens were taken as average value from at least 20 reading for each specimen. Surface morphologies and phase identifications of coated layers were studied using a SEM scan electron microscope fitted with EDX analyzer (SEM/EDX type: Thermo Scientific Quattro S) and X-Ray Diffraction device (XRD Simense D5000 powder difractometer Cu Kα radiation (wavelength= 0.154nm) with a nickel filter at 40 kv and 30 mA).

2.5. High temperature oxidation resistance

Cyclic high-temperature oxidation resistance of coated and uncoated specimens of chromium low alloyed steel was investigated by heating the specimens in furnace atmosphere at 500 ±10 °C for 72 hours using electrical resistance furnace. The specimens are weighed intermittently to determine the specific change in weight during the oxidation at 500 °C.

2.6. Electrochemical corrosion behavior

Electrochemical corrosion behavior was conducted for coated and uncoated specimens at room temperature via potentiodynamic device (SP-300). All the potentiodynamic tests of electrochemical corrosion were carried out at a cell which consists of a standard three-electrode system; the aluminized specimen which immersed in aqueous solution which used as a working electrode; the platinum electrode used as the counter electrode and saturated calomel electrode (SCE) as a reference electrode. The test specimens, used as a working electrode, were embedded in epoxy resin with 3.143 cm^2 exposed working area. Before starting electrochemical experiments, these aluminized specimens were immersed in 3%NaCl aqueous solution [19] for a period of time approximately 20 minutes to made stabilization of open circuit potential (OCP vs SCE). All samples polarization measurements were conducted at the applied potential within the -1.5 to -0.5 V range.

3. Results and Discussion

3.1. Microstructure features and phase identification

The thickness of coated layers on all measured specimen was found to be inhomogeneous. Figure (1) represents the relation between dipping time and the average layer thickness measured for steel samples after hot dipping in both aluminium (fig. 1-a) and aluminium-silicon eutectic (fig. 1-b) molten bathes.

The overall layer thickness of coated layer in all test conditions increases with the increase of time of dipping. The presence of silicon in molten bath drastically decrease the thickness of coating layer, which was formed at same experimental conditions, for example the average thickness of aluminium coating layer approaches 16 micrometers while the average thickness of aluminium-silicon eutectic coating layer approaches 5 micrometers after same dipping time (10 minutes) and same degree of super heat (100°C). The presence of silicon in molten bath have significant inhibiting effect on the growth rate of aluminized and intermetallic layers which confirm the Nichollos's assumption and some literatures which supposed that the silicon atoms can replace Al atoms in all the binary intermetallics of the Fe-Al system so the diffusion condition can be changed [15, 20, 21, 22, 23, 24].

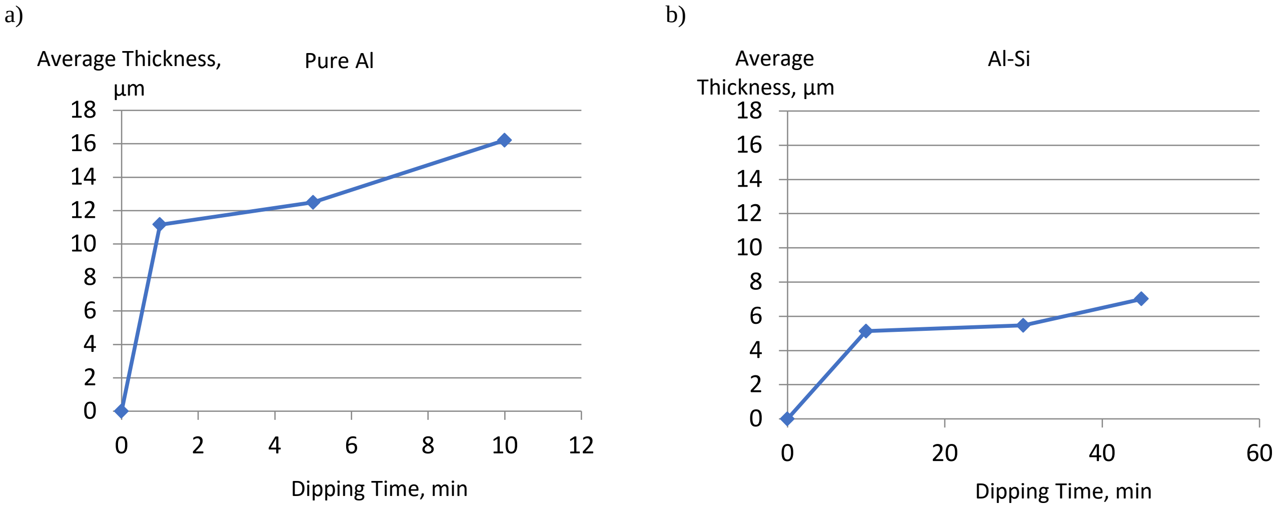

Fig. 1. The relation between dipping time (in min.) and the average thickness (in µm) of coated layer after hot dipping in molten Al (fig.

a) and in molten Al-Si eutectic bath (fig. b).

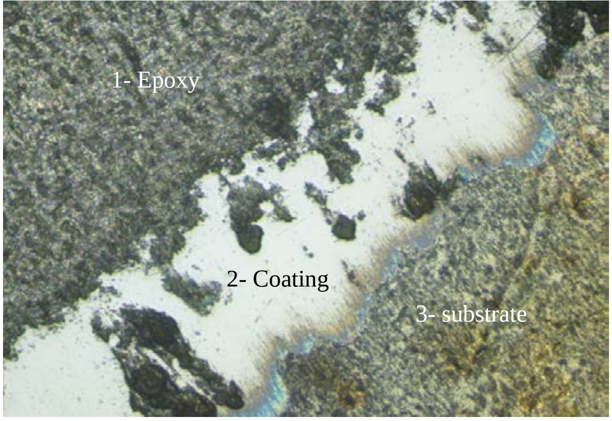
1- Epoxy
2- Coating
3- substrate

a)

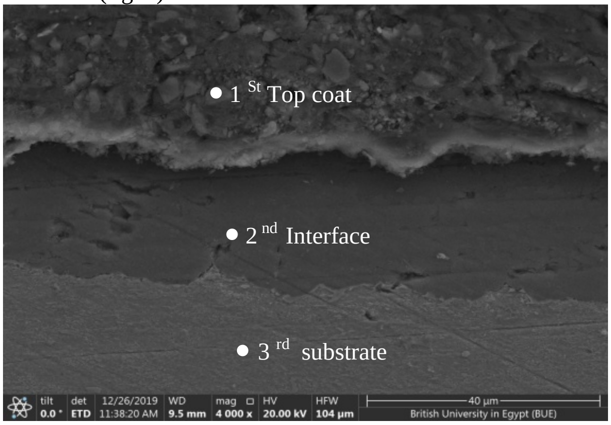
1 St Top coat
2 nd Interface
3 rd substrate
tilt 0.0 ° det ETD 12/26/2019 11:38:20 AM WD 9.5 mm mag 4 000 x HV 20.00 kV HFW 104 µm
40 µm
British University in Egypt (BUE)

b)

Fig. 2-a. Optical microstructure of Al coated steel after 30 min dipping time 1- Epoxy 2- Coating 3- Substrate. Fig. 2-b. SEM microstructure of Al coated steel after 30 min dipping time (4000x) 1- Top coat 2- Interface 3- The substrate

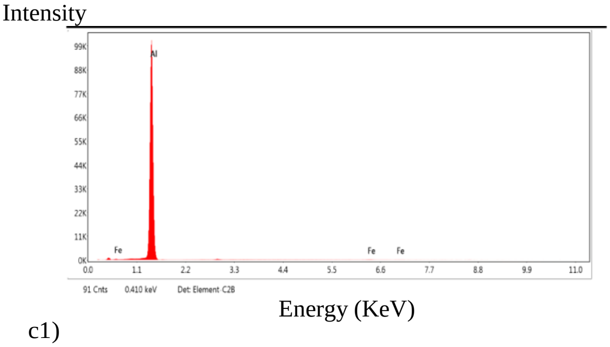

c1)

Fig. (2-c1). EDX analysis Point 1 (top coat)

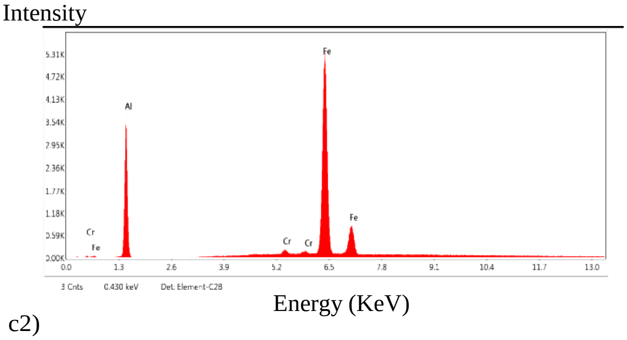

c2)

Fig. (2-c2). EDX analysis Point 2 (interface)

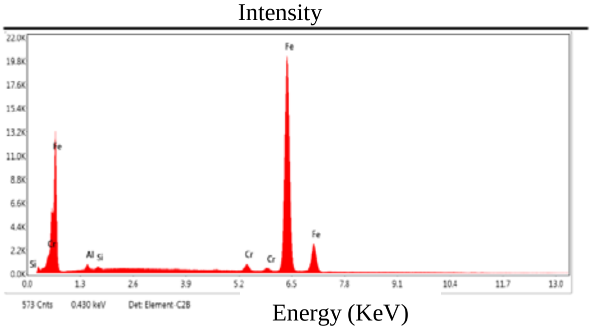

c3)

Fig. (2-c3). EDX analysis Point 3 (substrate)

Fig. (2-c). EDX analysis of Al coated steel after 30 min dipping time at different points (point 1 at the coating layer, point 2 at the interface and point 3 at substrate material

Table 4.

Results of EDX analysis for Al coated steel after 30 min dipping time at point 1, 2 and 3 in figure 2c

Element	Point 1 at top coating layer		Point 2 at interface		Point 3 at substrate	
	wt %	at%	wt %	at %	wt %	at%
Al	99.32	**99.67**	20.92	**35.35**	1.51	**3.06**
Fe	0.68	**0.33**	77.64	**63.39**	95.95	**93.7**
Si	-------	-------	1.44	1.26	0.66	1.27
Cr	-------	-------	-------	-------	1.88	**1.97**
AxBy				A_2B		

	Fe_3Al, FeAl

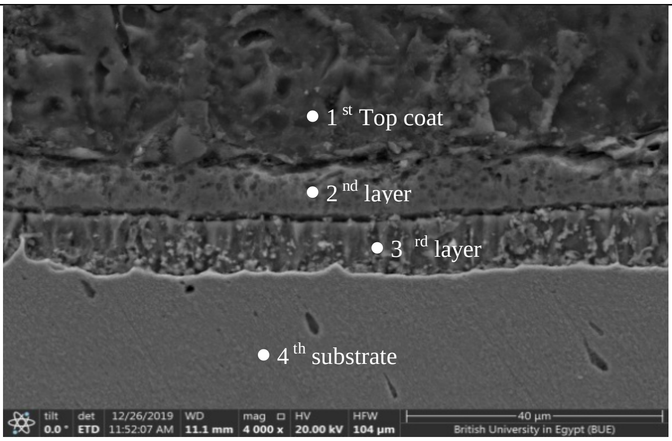
1 st Top coat
2 nd layer
3 rd layer
4 th substrate
a)
tilt 0.0 ° det ETD 12/26/2019 11:52:07 AM WD 11.1 mm mag 4 000 x HV 20.00 kV HFW 104 µm
40 µm
British University in Egypt (BUE)

Fig. (3-a). SEM microstructure of Al-Si coated steel after 30 min dipping time (4000x) 1- Top coat 2- 2nd sublayer interface 3- 3rd sublayer interface 4- The substrate

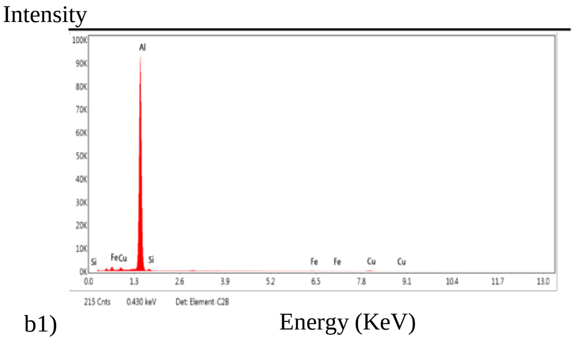

Fig. (3-b1). EDX analysis Point 1(top coat)

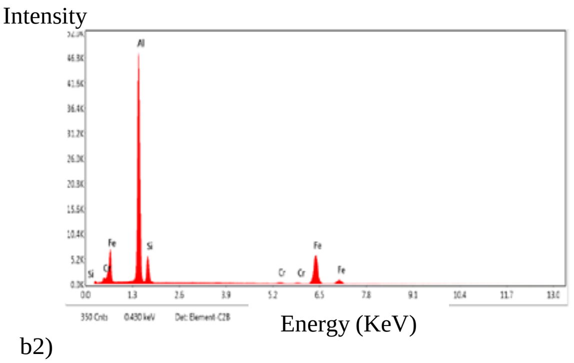

Fig. (3-b2). EDX analysis Point 2(coat/interface)

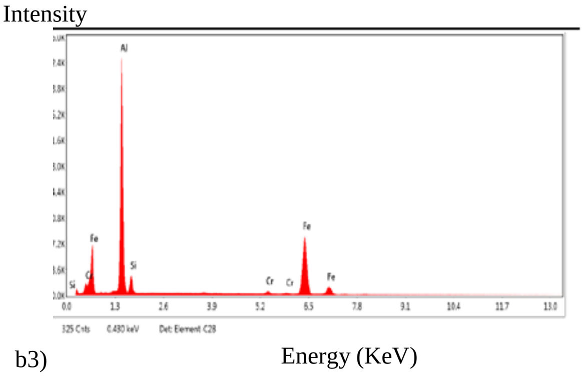

Fig. (3-b3). EDX Point 3 (interface/substrate)

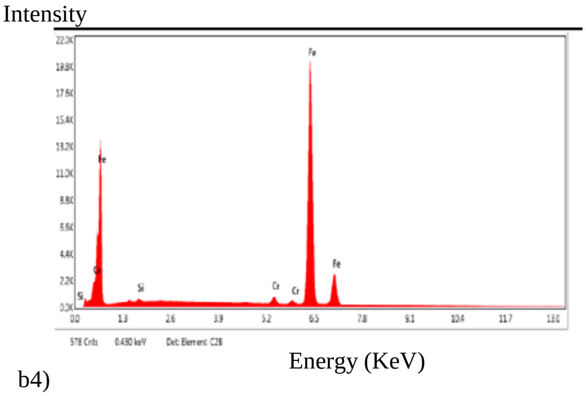

Fig. (3-b4). EDX analysis Point 4 (substrate)

Fig. (3-b). EDX analysis of Al-Si coated steel after 30 min dipping time at different points (point 1 at the coating layer, point 2 at the coat/interface, point 3 at interface/substrate and point 4 at substrate material

Table 5.
EDX numerical values of analysis at point 1, 2, 3 and 4 in the figure 3-b. (30 min dipping in Al-Si

Element	1st layer (topcoat)-point 1		2nd layer -point 2		3rd layer -point 3		4th Substrate point 4	
	wt. %	at%	wt. %	at. %	wt %	at %	wt %	at %
Al	94.96	96.76	57.21	69.17	48.1	63.77	-----	------
Fe	0.68	**0.32**	32.03	**18.71**	45.89	**29.39**	97.34	**96.51**
Si	1.87	**1.83**	10.05	**11.67**	4.61	**5.87**	0.72	**1.42**
Cu	2.52	1.09	----	----			----	----
Cr	----	**----**	0.71	**0.45**	1.4	**0.97**	1.94	**2.07**
AxByCz				Fe_2SiAl_7, $Fe(Al)_3Si$		Al_4Si_3Cr, Fe_2Al_5		

In order to study the nature of interphase and the possible reactions between substrate materials and coating layer, the interphase area was subjected to investigation using SEM, EDX and X-ray diffraction techniques. The test results of microstructural investigation are given in the figure 2 and 3. The detailed of EDX analyses are given in related charts (fig. 2c), (fig. 3b), table (4) and table (5).

The microstructures in (fig. 2-a) and (2-b) indicated that, after 30-minutes dipping time in molten aluminum bath, the interface boundary have irregular shape with serrated or tongue like morphology, while the interface bounder after same dipping time in molten Al-Si bath have relatively regular shape as it observed in (fig. 3-a). Such serrated morphology could be attributed to the anisotropic diffusion path throw the intermetallic layer during hot-dipping in aluminium bath [25]. Furthermore, the presence of silicon in molten bath restrict the inward diffusion of aluminum throw the substrate [26, 27].

The microstructures in (fig. 2-a), (2-b) for aluminum coated sample indicate the presence of two – layer, while three distinct layers with regular flat boundary lines were observed in SEM microstructure in (figure 3-a) after dipping on aluminum – silicon eutectic molten bath.

The results from EDX analysis are showed in tables (4) and (5) revealed that existence for several intermetallic phases present as results of inward diffusion alloying elements present in molten bathes and the outward diffusion of substrate alloying elements. There are five intermetallic phases are presented in binary equilibrium Fe-Al phase diagram are Fe_3Al, FeAl, $FeAl_2$, Fe_2Al_5 and $FeAl_3$, while more complicated intermetallic phases will be existing in actual systems depending on the bath composition, substrate material, dipping temperature, contact time and cooling rate

The mathematical analysis for EDX data in table (4) for Al coated sample reveled that the stochiometric atomic ratio between Fe and Al in point 2 are about Fe_2Al, which is not excite in the binary equilibrium phase diagram, it may be reflect the presence of Fe_3Al and FeAl mixture at the interface area. The analysis of EDX data point 1 and point 2 are not too far away from that of initial bath and substrate composition.

The results of EDX chemical analysis after hot dipping of chromium low alloy steel grade in molten Al-Si bath are given in (figures. 3-b) and summarized in tables (5), which reveal the existence of three chemically distinct sublayers overlaying the substrate materials. The EDX chemical analysis for the top layer at point number 1 has approximately the same chemical composition of commercially pure aluminum, that may be caused by inward migration of silicon to the next layer.

The EDX chemical analysis of 2nd layer at point number 2, indicates that iron diffuses outwardly while aluminum and silicon diffuse inwardly derived by difference in concentration gradient and chemical thermodynamic to form intermetallics between them. The stochiometric atomic ratio between Fe, Al and Si in point 2 may be reflect the presence of Fe_2SiAl_7 or $Fe(Al)_3Si$ intermetallic at the 2nd layer.

The EDX chemical analysis of 3rd layer at point number 3, indicates that the chromium diffuses outwardly from substrate material to the adjacent 3rd coating sublayer derived by concentration gradient. The stochiometric atomic ratio between Fe, Al, Si and Cr in point 3 may be reflect the presence of Fe_2Al_5 and Al_4Si_3Cr intermetallics at the 3rd layer.

The EDX chemical analysis of substrate material point 4 has approximately same chemical composition of original substrate material as given in table (1).

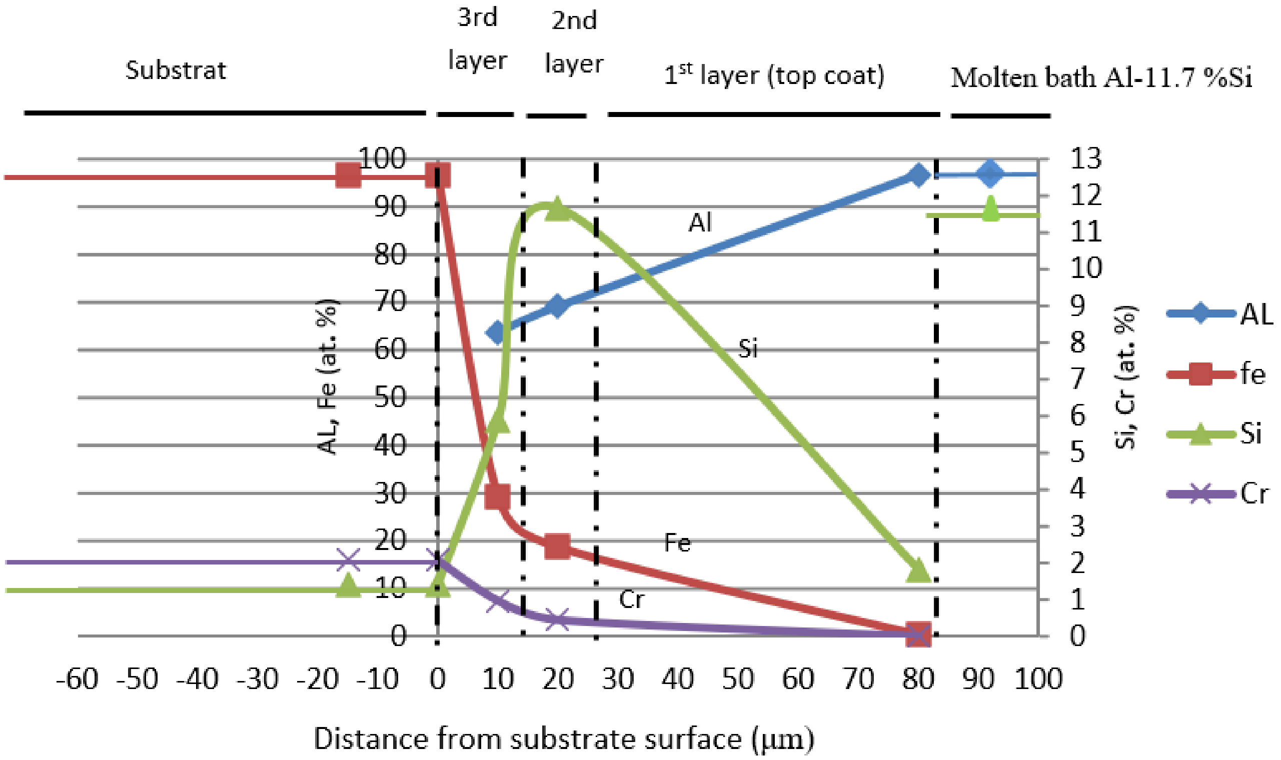

Fig. 4. Distribution of alloying element during hot dipping in Al-Si molten bath (data from the tab. 4 & fig 3-a)

Referring to diffusion baths shown in figure (4) it is clear that the silicon and aluminium diffused inward from the molten bath in the direction of the substrate surface. On the other hand, chromium and iron are diffused outward from the surface of the substrate material in the direction of the molten bath. It worth to be noted that Si highly concentrated at the 2nd sublayer which may be a sign to form an intermetallic.

In the light of EDX analysis in figure (4) and the published articles from [7, 16, 21] also referring to Fe-Al phase diagram the present intermetallics could be Fe_2SiAl_7 and/ or $Fe(Al)_3Si$ in the 2nd layer and Al_4Si_3Cr and/ or Fe_2Al_5 in the 3rd layer. The chemical affinity of silicon and the bath controlling parameters (bath temperature, dipping time and diffusion coefficient of Si in coating layer) are led to form intermetallics which is relatively high so the concentration of the silicon is high in the 2nd sublayer.

3.2. Thermal cyclic oxidation resistance

Thermal cyclic oxidation resistance of the coated and uncoated specimens of chromium low alloyed steel was investigated by heating the specimens in furnace atmosphere at 500 °C for 72 hours using electrical resistance furnace. The test results are given in figures (5) & (6), which represent the change in specimen weight during oxidation in (mg/cm^2) as a function of oxidation time in (hrs).

The test result from high-temperature cyclic oxidation in figures (5) & (6) showed that oxidation kinetics followed the parabolic rate law at test temperature for most tested samples.

The cyclic thermal oxidation resistance of all coated specimens was highly improved in comparison with that of uncoated specimens. After heating of specimens in oxidizing environment for 72 hours at 500 ºC, the specific gain in weight was strongly reduced from 121 mg/cm² for uncoated steel to 6 mg/cm² for Aluminum coated steel specimens after 10 minute dipping time and 5 mg/cm² for Al-Si eutectic coated steel specimens after 30 minute dipping time. Such similarities in high oxidation resistance of Al coated and Al-Si coated samples could be attributed to the chemical composition of the top coating layer in both cases, where protective oxide or oxides cover the outermost surface layer in both cases, as it explained in EDX discussion and analyses in (fig 2-c), (fig. 2-b), table (4) and table (5). The oxidation resistance of coated chromium low alloyed steel improved through preferential oxidation of aluminium atoms present in the top coating layer of steel substrate. Such high oxidation resistance of aluminized steel can be attributed to the formation of the impermeable passive protective aluminium- oxide layer of α-Al_2O_3, which is thermodynamically high stable.

At oxidation temperature, the inward diffusion of O^{2-} anions, the outward diffusion of all substrate cations addition to the bulk diffusivity of Al^{3+} cations occurred because of the concentration gradients and preferential chemical affinity [28, 29].

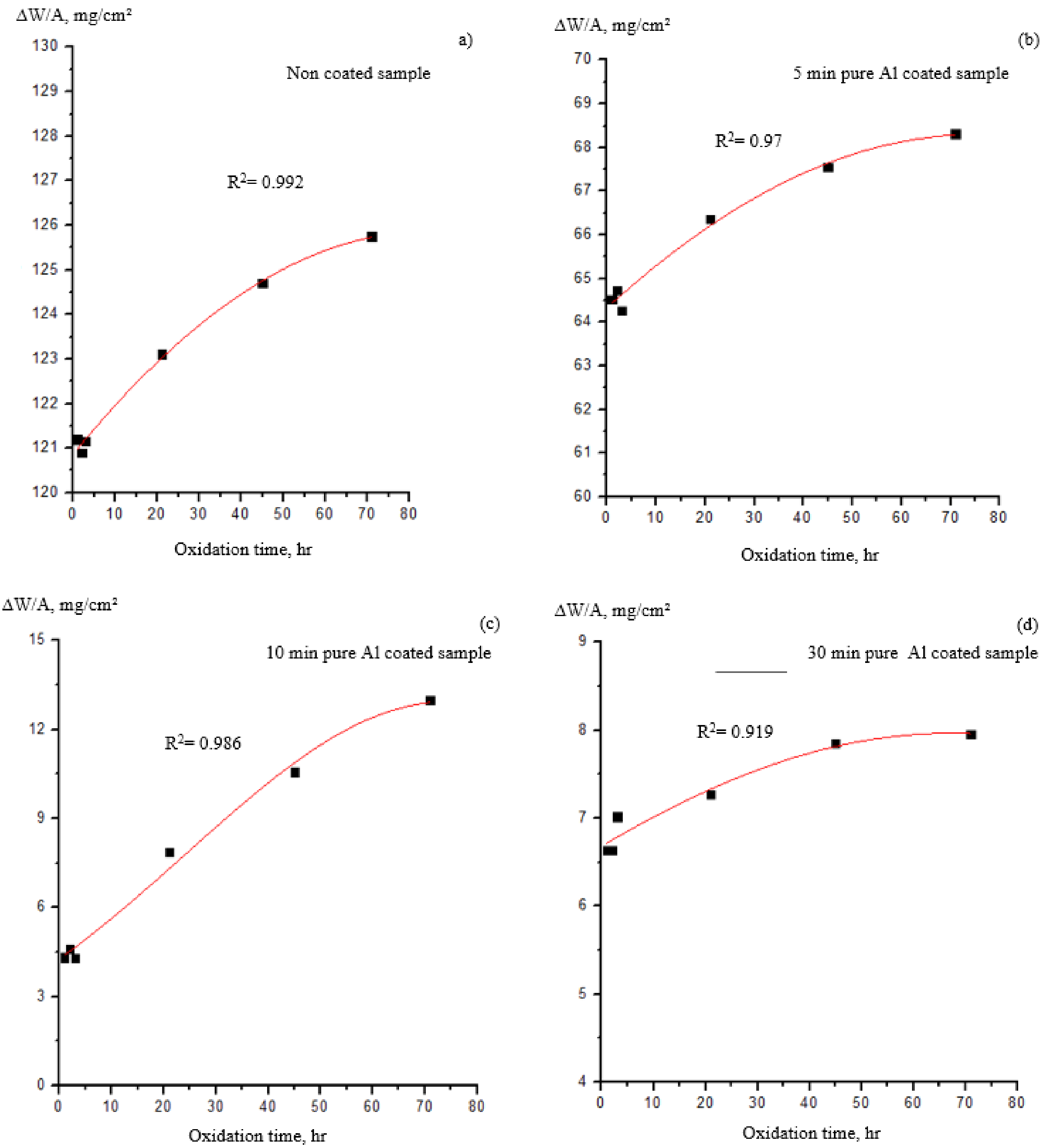

Fig. 5. the specific gain in weight mg/cm^2 during cyclic oxidation of uncoated and pure Al coated samples at different dipping time (a) Non coated sample b) 5 min pure Al coated sample (c) 10 min pure Al coated sample (d) 30 min pure Al coated sample

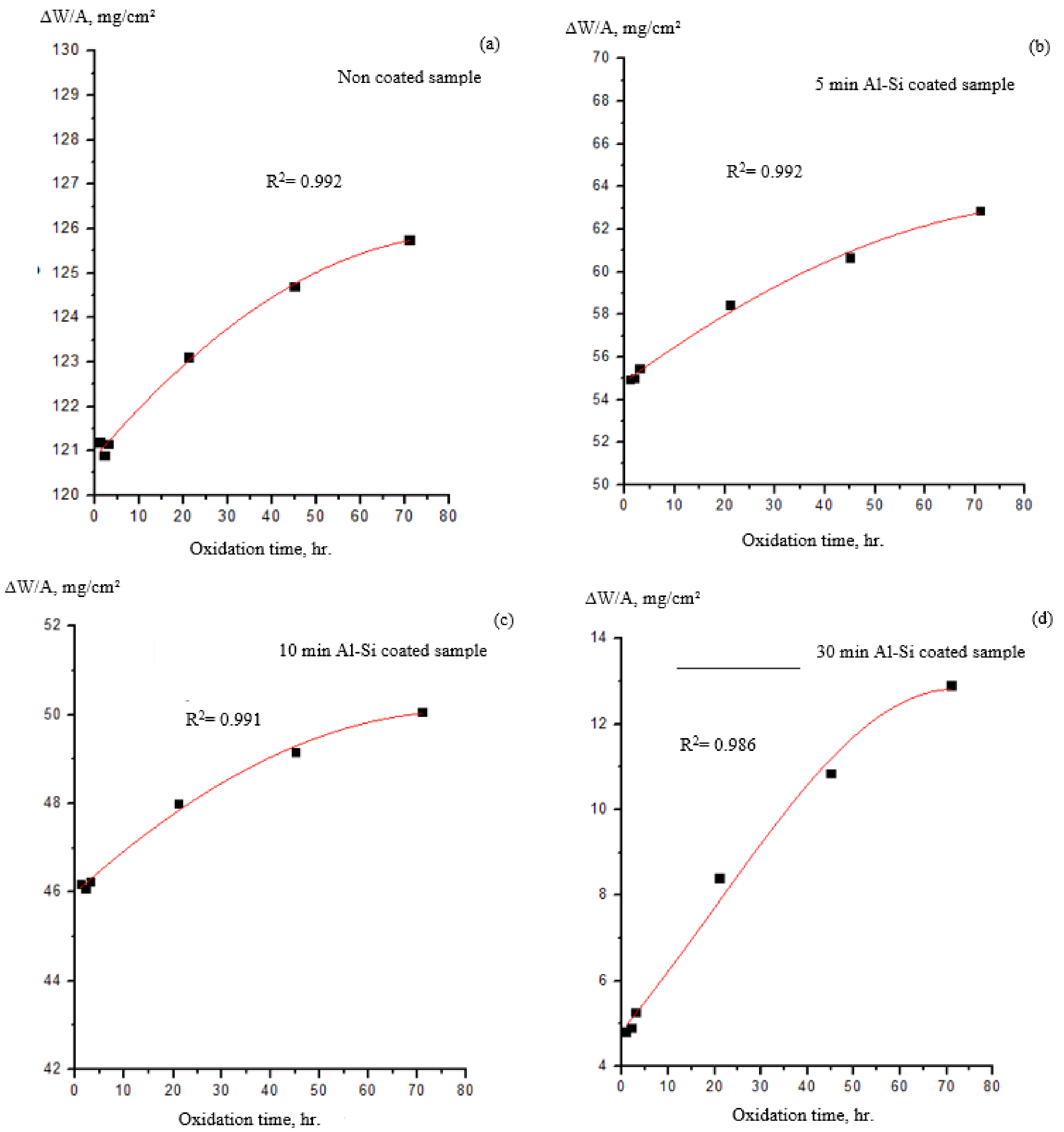

Fig. 6. the specific gain in weight mg/cm^2 during cyclic oxidation of uncoated and Al-11.7%Si coated samples at different dipping time (a) Non coated specimen (b) 5 min Al-Si coated sample (c) 10 min Al-Si coated sample (d) 30 min coated sample

The X ray diffraction in figure (7) and (8) shows the phases of aluminide coated specimens before and after oxidation at 500 °C for 72 hours. (Fig. 8-a) shows the presence of Al_2O_3 in the outer surface after oxidation test of Al coated samples, while (fig. 8-b) shows the presence of SiO_2 in the outer surface after oxidation test of Al-Si coated samples.

The results of XRD after hot dipping (fig. 7) and after oxidation (fig. 8) are not in agreement with results gained from EDX analysis for the same samples. The continues protective oxide or oxides at the top layer scale formed after high temperature oxidation of aluminum or aluminum and silicon in outermost layer is tight and very thin. This contradiction could be explained considering the analysis capability of both techniques. The EDX has a very low depth of analysis from 3 to 5 nm while XRD has much higher depth of analysis of a few micrometers.

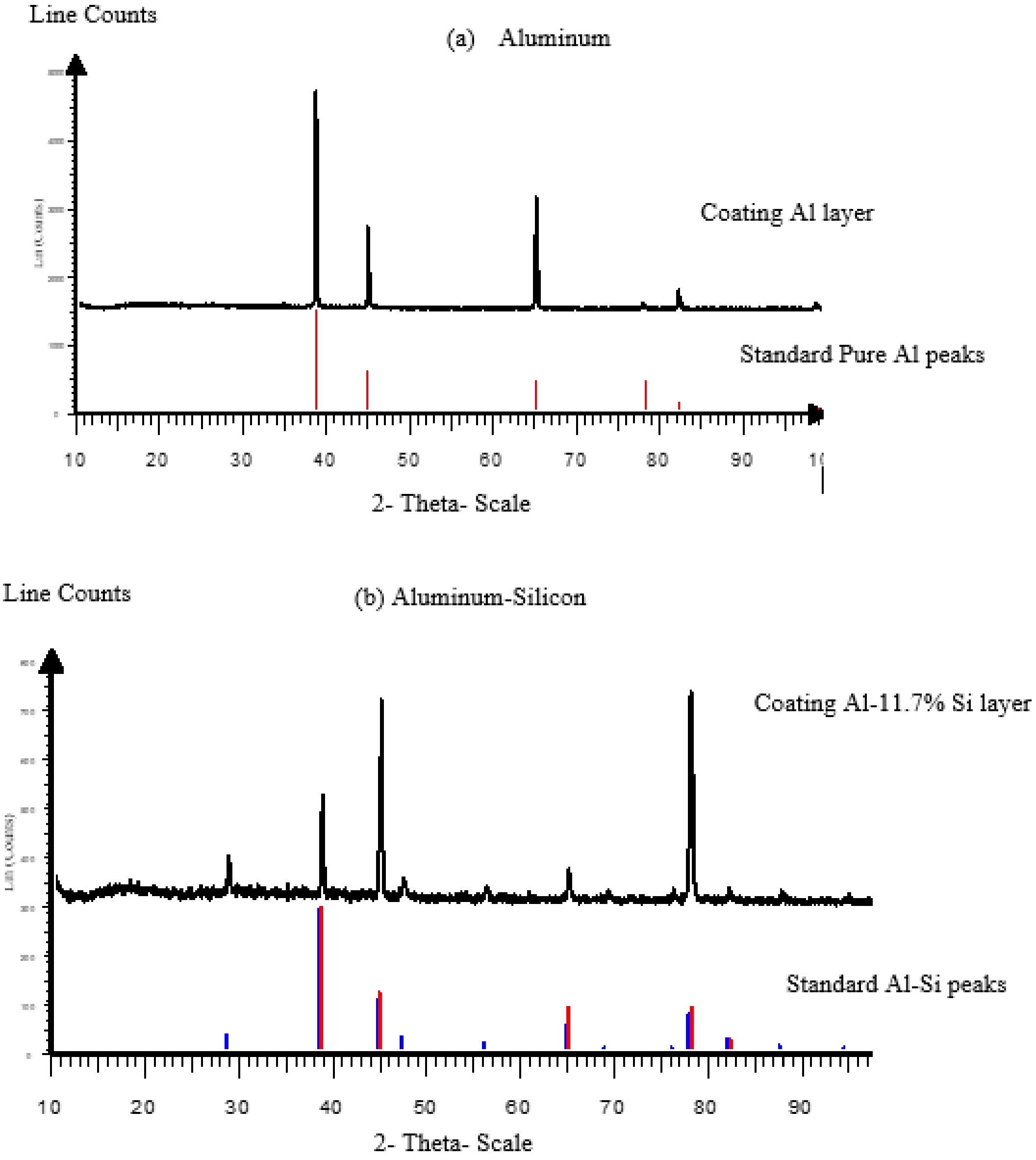

Fig. 7. XRD X- Ray Diffraction pattern for chromium low alloyed steel after hot dipping for 10-minutes in (a) Al and (b) Al-11.7%Si molten baths

(a) Aluminum

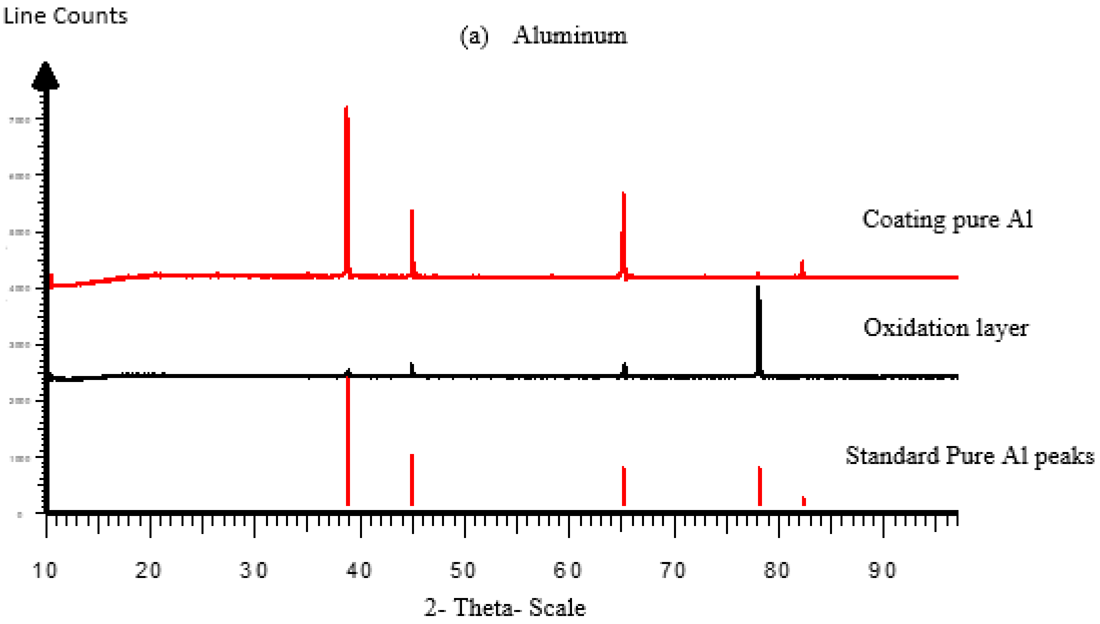

(b) Aluminum-Silicon

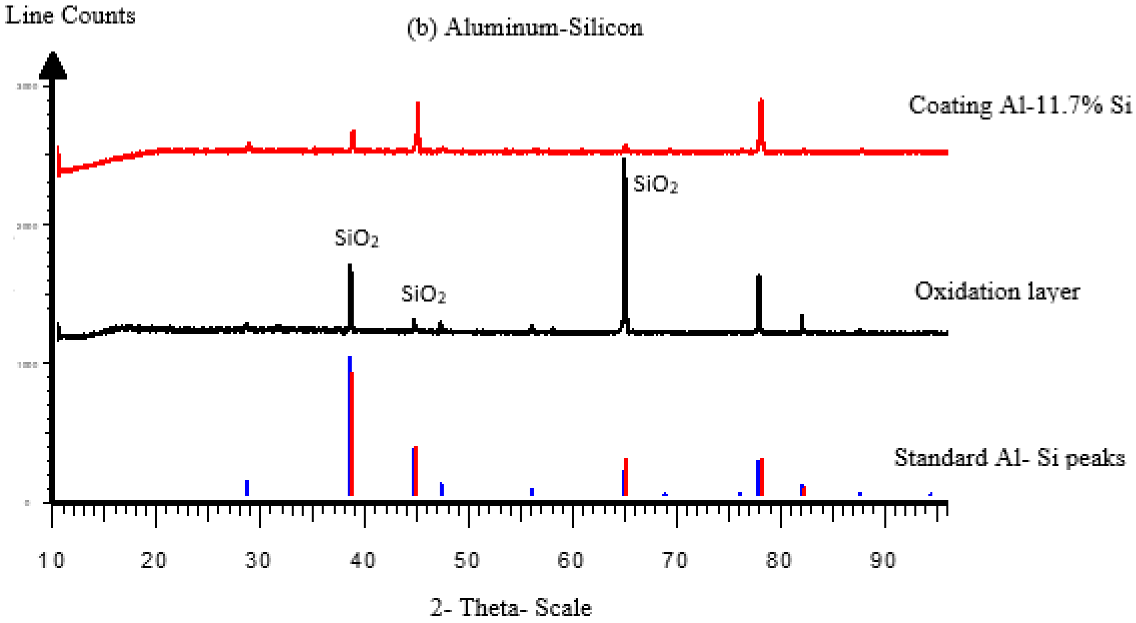

Fig. 8. XRD X- Ray Diffraction pattern after cyclic oxidation of coated samples at 500 ºC for 72 hours

3.3. Corrosion polarization

• uncoated • 5min. • 10min. • 30min. • 45min

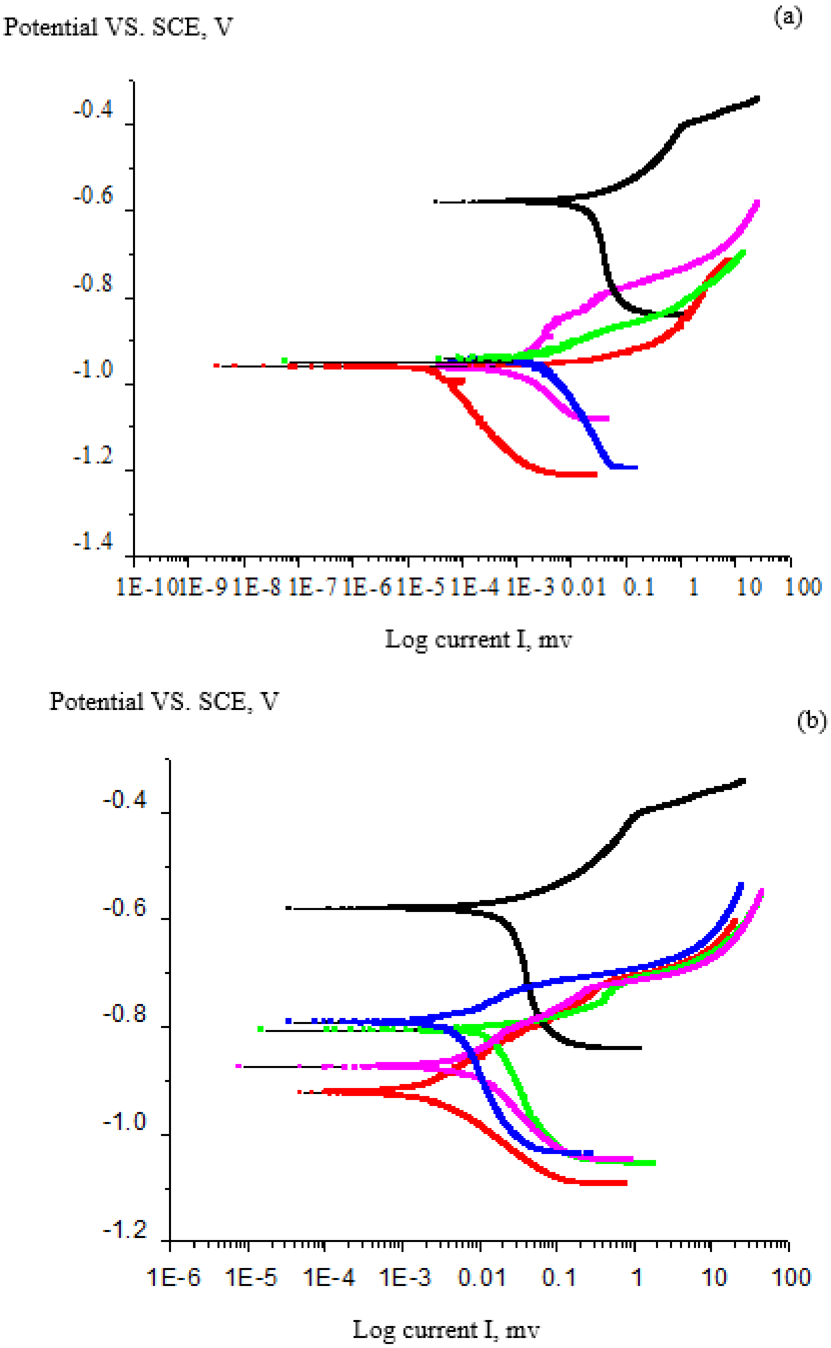

Fig. 9. Polarization curve for uncoated and coated samples after hot dipping at different dipping time. (a) in Al molten bath (b) in Al-11.7%Si molten bath

Table 6.
Corrosion polarization parameters for uncoated and coated specimens at different dipping time and different coating materials, (a) at commercially pure Al , (b) at Al-11.7%Si eutectic

a. Hot dipping in aluminium bath

Dipping time, min	βc mv/decay	Ba mv/decay	E corr mv	I corr. µA	Cor. Rat mmpy
0.0 min	628.7	121.8	-617	29.78	0.11
5	276.9	157.6	-1128	20.50	0.075
10	211.2	65.1	-966.55	4.84	0.017
30	118.4	102.4	-946.98	0.85	0.002
45	503.7	55.8	-886.98	3.15	0.010

b. Hot dipping in aluminium – silicon bath

Dipping time, min	βc mv/decay	βa mv/decay	E corr mv	I corr. µA	Cor. Rat mmpy
0.0 min	628.7	121.8	-616	29.784	0.11
5	103.8	69.3	-904	1.647	0.0057
10	282.4	50.9	-810	14.085	0.0488
30	131.7	79.4	-865	5.84	0.0202
45	289.0	26.9	-758	3.56	0.0124

(Figure. 9) and table (6) shows the results of Tafel polarization tests for chromium low alloyed steel before and after aluminizing. The corrosion current, i_{Corr}, was significantly decreased after the aluminizing process; however, the corrosion potential E_{Corr} after the aluminizing process was shifted to the active direction.

The result of Tafel analyses for both coating layers reveals that the corrosion rate decreased from 0.11mmpy for uncoated steel to 0.002 mmpy for aluminium coated steel after 30 minutes dipping time and to 0.005 mmpy for aluminium - silicon-coated steel after 5 minutes dipping time. Such decrease in the corrosion rate of all tested samples could be attributed to the formation of stable protective oxide or oxides at the surface of coated specimens, which will hinder the exposure of the steel substrate to the corrosive electrolyte and subsequently corrosion rate drastically reduced.

The different electrochemical corrosion behavior of coated samples at different dipping time, could be explained in the light of the possible diffusion and subsequent interaction between the substrate material and the aluminizing molten baths. Referring to both binary Al-Fe and ternary Al-Fe-Si phase diagrams, several intermetallic phases are possible to form as a result of hot dipping of steel samples in molten aluminizing bathes [27, 30].

In general, the nature and thickness of coating, intermetallic and interdiffusion layers formed through the interaction between substrate and molten bath, depends mainly on the dipping temperature and time besides the chemical composition of substrate material and molten bath.

4. Conclusion

- Hot dipping aluminizing is a successful method to improve oxidation and corrosion resistance of chromium low alloyed steel for both coating systems because the formation of thin protective oxide film in the outermost coating layer.
- It can be concluded that during different intervals of time, the layer thickness increased up to 16µm and 5µm for dipping in commercial pure Al and Al- 11.7%Si molten baths respectively at time interval 10 minutes.
- The gain in weight at high temperature cyclic oxidation was decreased by 24 times.
- The corrosion rate was decreased from 0.11 mmpy for uncoated specimen to be 2.9 $x10^{-3}$ mmpy for Aluminum coated steel and 5.7x 10^{-3} mmpy for Al-Si eutectic coated specimens.
- The presence of silicon in hot dipping molten bath inhabit the growth of coating intermetallic layers, decrease the total coating thickness and change the interface boundaries from tongue like shape to be more regular with flatter interface.
- Two distinct coating layers were observed after hot dipping aluminizing in Al bath, while three distinct layers were observed after hot dipping in Al-Si molten bath.
- The controlling parameters of hot dipping process (bath temperature, dipping time and diffusion coefficient of elements in coating layer) are led to the formation of intermetallics of type F_3Al and/ or FeAl in pure Al coated specimen and Fe_2SiAl_7 and/ or $Fe(Al)_3$ Si, Al_4Si_3Cr and/ or Fe_2Al_5 in Al-11.7%Si coated specimen.

Acknowledgement

The authors are thankful for the assistance of Dr Rehab El-Maghraby who helped to make corrosion polarization test at "OIL & GREEN CHEMISTRY RESEARCH CENTER."

References

[1] Kuruveri, U.B., Huilgol, P., Joseph, J. (2013). *Aluminising of mild steel plates*. ISRN Metallurgy. 1-6.

[2] Isiko, M.B. (2012). *Aluminizing of plain carbon steel: Effect of temperature on coating and alloy phase morphology at constant holding time*. Norway. Institute for material technology. 1-2.

[3] Davis, J.R. (1990). *Surface engineering.* vol. 5 of ASM Metals Handbook. Ohio, USA Materials Park.

[4] Ahmad, Z. (2006). *Principles of corrosion engineering and corrosion control*. London: UK. Elsevier. 17.

[5] Burakowski T., Weirzchok, T. (2000). Surface engineering of Metals- Principles, Equipments, Technologies. CRC Press, London, UK.

[6] Pattankude1, B.G., Balwan,. A.R. (2019). A review on coating process. *International Research Journal of Engineering and Technology (IRJET)*. 06(3), 7980.

[7] Huilgol, P., Bhat, S. & Bhat, K.U. (2013). Hot-dip aluminizing of low carbon steel using Al- 7Si-2Cu alloy baths. *Journal of Coatings.* 2013, 1-6.

[8] Lin, M.-B. Wang, C.-J. & Volinsky, A.A. (2011). Isothermal and thermal cycling oxidation of hot- dip aluminide coating on flake/spheroidal graphite cast iron. *Surface and Coatings Technology*. 206, 1595-1599.

[9] Dngik Shin, Jeong-Yong Lee, Hoejun Heo, & Chung-Yun Kang. (2018). Formation procedure of reaction phases in Al hot dipping process of steel. *Metals journal.* 1.

[10] Yu Zhang, Yongzhe Fan, Xue Zhao, An DU, Ruina Ma, & Xiaoming Cao. (2019). Influence of graphite morphology on phase, microstructure and properities of hot dipping and diffusion aluminizing coating on flake/spheroidal graphite cast iron. *Metals journal*. 1.

[11] Voudouris, N. & Angelopoulos, G. (1997). Formation of aluminide coatings on nickel by a fluidized bed CVD process. *Surface Modification Technologies* XI. 558-567.

[12] Wang, D. & Shi, Z. (2004). Aluminizing and oxidation treatment of 1Cr18Ni9 stainless steel. *Applied surface science*. Volume (227). 255-260.

[13] Murakami, K., Nishida, N., Osamura, K. & Tomota, Y. (2004). Aluminization of high purity iron by powder liquid coating. *Acta Materialia*. 52(5), 1271-1281.

[14] Cheng, W.-J. & Wang, C.-J. (2013). High-temperature oxidation behavior of hot-dipped aluminide mild steel with various silicon contents. *Applied surface science*. 274. 258-265.

[15] Mishra, B., Ionescu, M. & Chandra, T. (2013). The effect of Si on the intermetallic formation during hot dip aluminizing. *Advanced Materials Research*. Volume 922, 429-434.

[16] Kee-Hyun, *et. Al*. (2006). Observations of intermetallic compound formation of hot dip aluminized steel. *Materials Science Forum*. 519-521, 1871-1875.

[17] Fry, A., Osgerby, S., Wright, M. (2002). *Oxidation of alloys in steam environments.* United kingdom: NPL Materials Centre. 6.

[18] Scott, D.A. (1992). Metallography and microstructure in ancient and historic metals. London. Getty publications. 57-63.

[19] Lawrence J. Korb, Rockwell, David L. Olson. (1992). ASM Handbook Vol 13: *Corrosion: Fundametals, Testing and Protection*. Florida, USA: ASM International Handbook Committee.

[20] Nicholls, J. E. (1964). Corr. Technol. 11.16.

[21] Azimaee, H. *et. al*. (2019). Effect of silicon and manganese on the kinetics and morphology of the intermetallic layer growth during hot-dip aluminizing. *Surface and Coatings Technology*. 357. 483-496.

[22] Sun Kyu Kim, (2013). Hot-dip aluminizing with silicon and magnesium addition I. Effect on intermertallic layer thickness. *Journal of the Korean Institute of Metals and Materials*. 51(11), 795-799.

[23] Springer, H., Kostka, A., Payton, Raabe, D., Kaysser, A. & Eggeler, G. (2011). On the formation and growth of intermetallic phases during interdiffusion growth between low-carbon steel and aluminum alloys. *Acta Materialia*. 59, 1586-1600.

[24] Kab, M., Mendil, S. & Taibi, K. (2020). Evolution of the microstructure of intermetallic compounds formed on mild steel during hot dipping in molten Al alloy bath. *Metallography, Microstructure and Analysis*. Journal 4.

[25] Bahadur A. & Mohanty, O.N. (1991). Materials Transaction. *JIM*. 32(11), 1053-1061.

[26] Bouche, K., Barbier, F. & Coulet, A. (1998). Intermetallic compound layer growth between solid iron and molten aluminium. *Materials Science and Engineering A*. 249(1-2), 167-175.

[27] Maitra, T. & Gupta, S.P. (2002). Intermetallic compound formation in Fe–Al–Si ternary system: Part II. *Materials Characterization*. 49(4), 293-311.

[28] Nychka, J.A. & Clarke, D.R. (2005). Quantification of aluminum outward diffusion during oxidation of FeCrAl alloys. *Oxidation of Metals*. 63(Nos.5/6), 325-351.

[29] Lars, P.H. *et. All*. (2002). Growth kinetics and mechanisms of aluminum-oxide films formed by thermal oxidation of aluminum. *Journal of Applied Physics*. 92(3), 1649-1656.

[30] Murray, J.L. (1992). Fe–Al binary phase diagram, in: H. Baker (Ed.), Alloy Phase Diagrams. ASM International. OH- USA. Materials Park. 54.